Annexin IV Reduces the Rate of Lateral Lipid Diffusion and Changes the Fluid Phase Structure of the Lipid Bilayer When It Binds to Negatively Charged Membranes in the Presence of Calcium†

Rudolf Gilmanshin,‡,§ Carl E. Creutz,‖ and Lukas K. Tamm*,‡

Department of Molecular Physiology and Biological Physics and Department of Pharmacology, University of Virginia Health Sciences Center, Box 449, Charlottesville, Virginia 22908

Received December 13, 1993; Revised Manuscript Received May 9, 1994®

ABSTRACT: Bovine annexin IV (endonexin) was bound to supported planar bilayers composed of 1-palmitoyl-2-oleoylphosphatidylcholine (POPC) in the first monolayer facing the substrate, and varying mole fractions of POPC, 1-palmitoyl-2-oleoylphosphatidylglycerol (POPG) and small amounts of the fluorescent lipid analogs NBD-PC or NBD-PG in the second monolayer facing the large aqueous compartment. Lateral diffusion coefficients and mobile fractions of these phospholipids were measured by fluorescence recovery after photobleaching (FRAP) as a function of protein concentration and lipid composition in the presence of 2 mM $CaCl_2$ or 1 mM EDTA. In the absence of annexin IV, the lateral diffusion coefficients depended only little on the POPC:POPG ratios and were approximately 3.0 $\mu m^2/s$ for NBD-PG (no Ca^{2+}), 2.5 $\mu m^2/s$ for NBD-PG (2 mM Ca^{2+}), and 1.6 $\mu m^2/s$ for NBD-PC (with or without 2 mM Ca^{2+}). In the presence of 2 mM Ca^{2+} these diffusion coefficients decreased as a function of the added annexin concentration. A transition from a state with "rapid" lipid diffusion to a state with "slow" lipid diffusion occurred at about 80 nM annexin IV and was independent of the POPC:POPG ratio. In addition to reducing the lipid lateral diffusion coefficients, annexin IV also gave rise to two-component lateral diffusion of the lipids in these mixed bilayers. The split of the single diffusion coefficient of NBD-PG into two components occurred at most POPC:POPG ratios upon binding of annexin IV, but required higher annexin concentrations at mole fractions of POPC between 66 and 82 mol % than at high mole fractions of POPG or 90 mol % POPC. The magnitude of the decrease of both lateral diffusion coefficients depended strongly on the amount of POPG in the membrane, ranging from a 0.8- and 1.6-fold decrease at 10 mol % POPG to a 5- and 35-fold decrease for the higher and lower diffusion coefficient, respectively, at 99 mol % POPG. Since similar results were obtained with the NBD-PG and NBD-PC lipid probes, it is concluded that in the presence of Ca^{2+} annexin IV induces a fluid–fluid phase separation in these membranes in a POPG-dependent fashion rather than forming long-lived stoichiometric complexes with the POPG molecules.

Annexins are a family of proteins that bind to phospholipid bilayers in a calcium-dependent manner. Some members of this family appear to be involved in membrane-to-membrane fusion and exocytosis, either by direct membrane interactions or indirectly in a regulatory pathway. Other functions may include interactions with cytoskeletal proteins, anticoagulant activities, and the inhibition of phospholipase A_2. All annexins, except annexin VI (which consists of eight repeats), have four highly homologous repeats of about 70 amino acid residues each [see Creutz (1992) for a recent review]. From the three-dimensional crystal structures of annexins I and V (Huber et al., 1990, 1992; Concha et al., 1993; Weng et al., 1993) it is evident that each repeat folds into a bundle of four antiparallel helices that is each topped off with a fifth perpendicular helix. The circular arrangement of these four domains exposes multiple calcium binding sites on the same side of the disk-shaped molecule and creates a narrow hydrophilic channel through its center. The main differences between the individual members of the family are variations in the N-terminus, which, in the annexin I and V structures, is located on the opposite side of the molecule from the calcium binding sites.

The various modes of lipid interactions of the annexins have been the subject of several previous studies. Although there are still conflicting views about the precise lipid requirements of several of the annexins, it appears that some require negatively charged lipids or phosphatidylethanolamines for high-affinity membrane binding. For example, the calcium concentration needed for half-maximal binding of annexin V to planar bilayers of cardiolipin, DOPG,[1] DOPS, soybean PI,

† Supported by NIH Grant R01 AI30557 to L.K.T.

* Corresponding author.

‡ Department of Molecular Physiology and Biological Physics.

§ Permanent address: Institute of Mathematical Problems of Biology, Russian Academy of Sciences, Pushchino, Moscow Region, 142292 Russia.

‖ Department of Pharmacology.

® Abstract published in *Advance ACS Abstracts*, June 15, 1994.

[1] Abbreviations: *D*, lateral diffusion coefficient; DOPA, dioleolyl-3-*sn*-phosphatidic acid; DOPC, dioleolyl-3-*sn*-phosphatidylcholine; DOPE, dioleolyl-3-*sn*-phosphatidylethanolamine; DOPG, dioleolyl-3-*sn*-phosphatidylglycerol; DOPS, dioleolyl-3-*sn*-phosphatidylserine; EDTA, ethylenediaminetetraacetic acid; EGTA, ethylene glycol bis(β-aminoethyl ether)-*N*,*N*,*N*′,*N*′-tetraacetic acid; FRAP, fluorescence recovery after photobleaching; LB, Langmuir–Blodgett; mf, mobile fraction; NBD-PA, 1-acyl-2-[12-[(7-nitro-2,1,3-benzoxadiazol-4-yl)amino]dodecanoyl]-3-*sn*-phosphatidic acid; NBD-PC, 1-acyl-2-[12-[(7-nitro-2,1,3-benzoxadiazol-4-yl)amino]dodecanoyl]-3-*sn*-phosphatidylcholine; NBD-PG, 1-acyl-2-[12-[(7-nitro-2,1,3-benzoxadiazol-4-yl)amino]dodecanoyl]-3-*sn*-phosphatidylglycerol; PC, total phosphatidylcholine (labeled and unlabeled) in the lipid mixture; PE, phosphatidylethanolamine; PG, total phosphatidylglycerol (labeled and unlabeled) in the lipid mixture; PI, phosphatidylinositol; POPC, 1-palmitoyl-2-oleoyl-3-*sn*-phosphatidylcholine; POPG, 1-palmitoyl-2-oleoyl-3-*sn*-phosphatidylglycerol; PS, phosphatidylserine; SDS, sodium dodecyl sulfate; SPB, supported planar bilayer.

0006-2960/94/0433-8225$04.50/0

DOPA, DOPE, and sphingomyelin increases in this order (Andree et al., 1990). In mixed bilayers of DOPS and DOPC the calcium concentrations required for half-maximal binding of annexin V decreased with increasing PS:PC mole ratios. Subsequently, it was found that the binding of annexins V and VI to lipid membranes was sensitive not only to negatively charged lipids but also to the nature of the zwitterionic lipid matrix in which the negatively charged lipids were inserted. Egg PE strongly promoted calcium-dependent annexin binding compared to egg PC in mixed vesicles with 20 mol % bovine brain PS (Bazzi et al., 1992). Variation of the PS:PE ratio showed that 20 mol % PS provided optimum conditions and was as effective as 100% PS for the binding of annexins V and VI. Annexin VI also appears to cluster the negatively charged lipid NBD-PA (15 mol %) in egg PC and egg PE bilayers upon membrane binding (Bazzi & Nelsestuen, 1991, 1992). The extent of clustering is identical in both lipid matrices, but the kinetics of cluster formation and cluster dissolution are much slower in PE than in PC. Lipid clustering was also induced when annexin IV was bound to lipid vesicles that were composed of 5 or 10 mol % pyrene-labeled PG in a background of bovine liver PC (Junker & Creutz, 1993).

In addition to binding to membranes, some annexins have the ability to self-associate on membrane surfaces. This property may be regulated by the N-terminal domains of the annexins which distinguish the different annexins from each other. Annexin self-association on membrane surfaces may also be functionally important for the proposed physiological role of some annexins in exocytosis, where they are thought to be involved in the docking and fusion of exocytotic vesicles with the plasma membranes of secretory cells (Creutz, 1992). For example, annexin V has the shortest N-terminus of all annexins and does not self-associate in solution, but forms trimeric units on negatively charged phospholipid vesicles (Concha et al., 1992). Annexin VII (synexin) which has an extended tyrosine-rich N-terminus appears to self-associate in solution and on the surface of chromaffin granule membranes in the presence of Ca^{2+} (Zaks & Creutz, 1991). Annexins IV–VI crystallize in a triskelion pattern on lipid monolayers (Newman et al., 1989, 1991; Mosser et al., 1991). Finally, it has also been shown that several annexins can promote the fusion of lipid model membranes (Meers et al., 1988, 1991, 1992). However, in all cases that were investigated, the annexins appeared to accelerate the rate of the vesicle aggregation reaction rather than the fusion event per se.

Taken together, it appears from these studies that the lipid-phase and domain structure can play an important role in the mechanism of annexin-mediated membrane-to-membrane binding and, perhaps, membrane fusion. In this study, we investigate changes in the dynamic structure of mixed-lipid bilayers composed of POPC and POPG in response to the calcium-dependent binding of annexin IV by lateral diffusion measurements using the technique of fluorescence recovery after photobleaching (FRAP). Similar to Andree et al. (1990) who used planar membranes for their ellipsometric measurements, we use single supported planar bilayers (Tamm & McConnell, 1985) as the preferred model system for our lateral diffusion measurements. We find that the binding of annexin IV reduces the lateral diffusion coefficients of the lipids as a function of the POPG concentration in the membranes and that PC- and PG-derived lipid probes report very similar diffusion coefficients in membranes which are otherwise identical in composition.

MATERIALS AND METHODS

Materials. NBD-PC, NBD-PG, POPC, and POPG were purchased from Avanti Polar Lipids, Inc. (Alabaster, AL) and used without further purification. Both fluorescent lipid analogs had the NBD label attached to the methylene segment in position 12 of the *sn*-2 chain. All other chemicals were from Sigma (St. Louis, MO) or Fisher (Fair Lawn, NJ) and were of the highest available purity.

Bovine annexin IV (endonexin) was expressed in *Escherichia coli* and purified as outlined here and described in detail by Nelson (1993). The bovine cDNA (Hamman et al., 1988) was modified by site-directed mutagenesis to introduce an *Nco*I restriction site at the initiation codon. The coding sequence was then subcloned into the "ATG" vector pET11d (Studier et al., 1990). In this vector annexin expression is under control of a T7 promoter sequence. T7 RNA polymerase is expressed under control of a lac promoter in the appropriate host strain (BL21DE3). The full-length protein of native amino acid sequence is produced. The purification of the recombinant protein relied on calcium-dependent binding to bovine brain lipids (Creutz et al., 1991). The protein obtained by this procedure was further purified by gel filtration on a Superose 12 FPLC column (Pharmacia, Piscataway, NJ). The elution buffer was 10 mM Tris-HCl, pH 7.5, and 0.1 M NaCl containing 0.02 mM EDTA. This step was found to be important to remove lipid contaminants that competed for the lipids in the planar bilayers in the annexin binding reaction. The resulting material ran as a single major peak when rechromatographed on the Superose 12 column and produced a single band at approximately 32 kDa on SDS–polyacrylamide gels. Concentrations of the annexin IV stock solutions were determined by absorption spectroscopy using a molar extinction coefficient of 25 100 M^{-1} cm^{-1} at 278 nm (M. Junker, personal communication). After gel filtration, no correction for light scattering was needed. Solutions of purified annexin were immediately frozen and stored in small aliquots at −18 °C. The accuracy of the annexin IV concentrations of the diluted solutions for the measurements is estimated to be ±4%.

Preparation of Supported Planar Bilayers. SPBs were formed on the surface of oxidized silicon wafers (The International Wafer Service, Portola Valley, CA) by the Langmuir–Blodgett technique as described (Tamm, 1988). The first monolayer was 100% POPC in all samples. The second monolayer was composed of POPC and POPG and contained small amounts (0.7–1.5 mol %) of NBD-PC or NBD-PG, as indicated. Changing the fluorescent probe concentration in this range did not influence any of the conclusions drawn in this paper. The subphase for all monolayer depositions was 0.01 M Tris–acetic acid, pH 5.0, and a surface pressure of 32 mN/m was maintained during transfer. The first monolayer was transferred by conventional vertical LB deposition, and the second monolayer was deposited by pushing the coated substrate through the air–water interface horizontally (Tamm & McConnell, 1985). A glass cover slip was attached to the substrate with double-stick tape under water. Buffers were exchanged by flushing at least 240 μL of the desired solutions through the space between the SPB and the cover slip, the volume of which varied between 25 and 40 μL in different samples. The SPBs were never exposed to air by this treatment. The *relative* accuracies of each lipid concentration in mixed lipid bilayers are estimated to be ±5%, i.e., a mole percentage quoted as 20% may actually vary between 19 and 21%.

Fluorescence Recovery after Photobleaching. Lateral diffusion coefficients and mobile fractions of the NBD-labeled

lipid analogs in the bilayer were determined by FRAP in the epi-illumination, pattern photobleaching mode as described (Kalb et al., 1992; Tamm & Kalb, 1993). The periodic stripe pattern was produced by focusing a Ronchi ruling in the back-focal image plane according to Smith and McConnell (1978). To measure the diffusion coefficients on different length/time scales, Ronchi rulings of 25, 50, 75, and 125 lines per inch were used which resulted in stripe periods, p, of 25.4, 12.7, 8.47, and 5.08 μm on the sample, respectively. A 40× water immersion objective (Carl Zeiss, Thornwood, NY) was used in all experiments. In our new FRAP instrument the microscope is an Axiovert 35 (Zeiss) and the argon ion laser is an Innova 300-4 (Coherent, Palo Alto, CA). All other components of the instrument are as previously described (Tamm, 1988; Kalb et al., 1992). Individual FRAP curves were fit by nonlinear Marquardt routines (ASYST software, Keithley Instruments, Taunton, MA) to one or two exponentials using the following equation:

$$F(t) = F_\infty - A_1 \exp(-D_1 a^2 t) - A_2 \exp(-D_2 a^2 t) \quad (1)$$

where $a = 2\pi/p$, F_∞ is the fluorescence intensity at a long time after bleaching, A_1 and A_2 are the amplitudes, and D_1 and D_2 are the translational diffusion coefficients of the fast and slow components, respectively. For single-exponential fits, A_2 is set equal to zero. The mobile fractions of each component are calculated by

$$\mathrm{mf}_1 = A_1/(F_{\mathrm{pre}} - F_0) \times 200 \quad (2a)$$

$$\mathrm{mf}_2 = A_2/(F_{\mathrm{pre}} - F_0) \times 200 \quad (2b)$$

where $A_1 + A_2 = F_\infty - F_0$, F_{pre} is the fluorescence intensity before the bleach pulse, and F_0 is the fluorescence intensity immediately after the bleach pulse. $\mathrm{mf}_1 + \mathrm{mf}_2$ was 85–100% in all experiments reported in this work, implying that no or only small immobile fractions were observed. Typically, six different spots were measured on each sample and under each condition. In most experiments, the averaged values of several independently prepared samples were averaged. The error bars include the standard deviations originating from sample and spot variations and were calculated with standard error propagation laws. In those cases where only one sample was used (some protein titration experiments), we nevertheless included in the error bars typical errors for sample-to-sample variation, because these errors are typically larger than those originating from spot-to-spot variation. All measurements were conducted at room temperature (21–23 °C).

Experimental Scheme. The following standard scheme of sequential FRAP measurements under various conditions was adopted for most experiments. The SPB was first thoroughly washed with buffer (10 mM Tris-HCl, pH 7.5, 0.1 M NaCl) containing 1 mM EDTA to eliminate any possible contamination of the sample by bivalent ions. A first set of diffusion measurements was made in this solution. Next, the SPB was treated with buffer containing 2 mM $CaCl_2$, and lateral lipid diffusion was measured in this solution. The sample buffer was then exchanged with 240 μL of annexin IV at the desired concentration (four consecutive aliquots of 60 μL were flushed through the sample). $CaCl_2$ (2 mM) was added to the protein solution immediately before it was added to the membrane. To control for the possible effects of annexin self-association under these conditions, some samples of annexin IV were preincubated with Ca^{2+} for up to 1 h, before they were added to the SPBs. No significant difference was observed between these and the standard samples. The sample was then incubated for 30–90 min (depending on the protein concentration; the higher concentrations needed less time for equilibration). FRAP experiments were carried out in the presence of bound annexin IV. To ascertain that an annexin binding equilibrium had been reached, the annexin solution was replaced with a fresh annexin solution and incubated for 30–60 min, and the sample was remeasured. Except for very small annexin concentrations with membranes of low POPG content, the results of the diffusion measurements were the same after the first and second incubation. In those cases where the results after the first and second addition of annexin were not the same, the membranes were incubated for a third time with a fresh annexin solution and remeasured. Equilibrium was always reached under these conditions, and the average D and mf values of the second and third annexin IV additions are reported in these cases.

Usually, another similar cycle of measurements was carried out with a different annexin IV concentration using the same SPB preparation. We found that, within experimental error, there was no difference between the values measured with "used" or freshly prepared samples, if the second protein concentration was at least 2 times greater than the previous one. Finally, annexin IV was dissociated from the membrane and washed out from the sample with the buffer containing 1 mM EDTA. The sample was treated with the buffer containing 2 mM $CaCl_2$, and two final sets of FRAP experiments were carried out under Ca^{2+}-free and Ca^{2+}-containing conditions, respectively.

RESULTS

Lipid Diffusion in the Absence of Annexin IV. To understand the effect of annexin IV binding on the lateral diffusion of lipids in supported planar bilayers, it was necessary to first obtain accurate measurements of the lateral diffusion coefficients and mobile fractions of the lipids in the absence of annexin IV, but in the presence of either 1 mM EDTA or 2 mM $CaCl_2$. These experiments were carried out before the addition of annexin IV and after the dissociation of membrane-bound annexin IV with EDTA. Panels A and B of Figure 1 show two typical FRAP curves of bilayers of 22 mol% POPC, 76.5 mol % POPG, and 1.5 mol % NBD-PG or NBD-PC, respectively, in the presence of 2 mM $CaCl_2$. Both curves were fit to single exponentials. The calculated lateral diffusion coefficients and mobile fractions were 2.4 ± 0.1 and 1.4 ± 0.1 $\mu m^2/s$ and 97 ± 2% and 95 ± 2%, respectively. In the presence of 1 mM EDTA, the corresponding values of D and mf were 3.0 ± 0.1 and 1.7 ± 0.1 $\mu m^2/s$, and 97 ± 2% and 97 ± 2%. These results are in good qualitative agreement with those measured in similar systems, but with a different FRAP instrument (Tamm, 1988; Kalb et al., 1992). The somewhat faster diffusion rate of the NBD-labeled negatively charged PG lipid analog compared to that of the zwitterionic PC lipid analog in an otherwise identical lipid bilayer may be due to a diffusion enhancement by charge repulsion which seems to be partially screened by 2 mM Ca^{2+}. One may expect that, around charged lipids, excluded areas exist which are not available for diffusion of charged lipids of the same sign. This would decrease the effective mean free path and increase the apparent lateral diffusion coefficient of such lipids.

There is another interesting feature which distinguishes NBD-PG from NBD-PC diffusion in these samples: The NBD-PG data are well fit by a single-exponential recovery, as can be seen from the residuals between the data and the fit that are plotted in the inset of Figure 1A. However, with NBD-PC, we observed a small, but well-defined, deviation

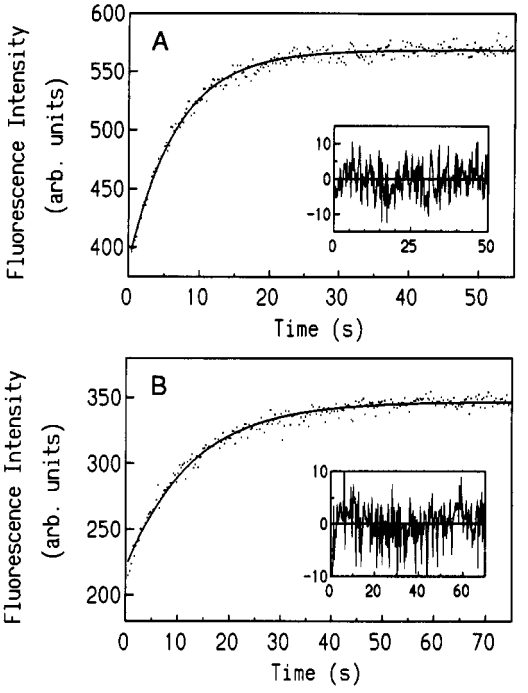

FIGURE 1: FRAP experiments measuring lipid diffusion in supported planar bilayers in which the second lipid monolayer was composed of 22% POPC, 76.5% POPG, and 1.5% NBD-PG (A) and 22% POPC, 76.5% POPG, and 1.5% NBD-PC (B). The lines represent the best fit single exponential curves to the experimental data. The insets show the residuals between the experimental data and the fitted curves. The resulting lateral diffusion coefficients and mobile fractions were 2.40 $\mu m^2/s$ and 100% in (A) and 1.30 $\mu m^2/s$ and 93% in (B). A 25-lines-per-inch Ronchi ruling was used. The buffer was 10 mM Tris-HCl, pH 7.5, 0.1 M NaCl, and 2 mM $CaCl_2$.

from a single-exponential fit. The residuals of all FRAP measurements with NBD-PC exhibited a long-range wave around the zero line (Figure 1B, inset). A better fit of the data of Figure 1B could be obtained with a double-exponential function (eq 1) corresponding to two lipid components with diffusion coefficients of 0.9 ± 0.3 and 3.4 ± 1.2 $\mu m^2/s$, and mobile fractions of 55 ± 19% and 45 ± 19%, respectively. The residuals of the double-exponential fit produced random noise around the zero line (not shown), indicating a good fit of the data to this function. The numerical values of the two diffusion coefficients are quite close to each other, and their resolution is just above the noise level. Therefore, the error margins on the amplitudes of the two exponentials (i.e., the two mobile fractions) are quite large. Very similar results were obtained in the presence of 1 mM EDTA. We consistently observed two-component lateral diffusion in supported membranes when NBD-PC was used as the fluorescent probe, but a fit with a single-component lateral diffusion was sufficient whenever the probe was NBD-PG.

Lateral diffusion coefficients were measured as a function of lipid composition (POPC and POPG) in the supported bilayers with both probes in the presence of either 2 mM $CaCl_2$ or 1 mM EDTA. These data are presented in Figures 2 and 3. In Figure 2 all data were fit to a single exponential function. The lateral diffusion coefficients were quite independent of the lipid composition in the range from 0 to 80 mol % total PC, but they were increased by a small amount at the higher PC contents in the bilayer. The same general trends were observed for the NBD-PG and NBD-PC probes in the absence and presence of Ca^{2+}. The data of NBD-PG diffusion in supported bilayers could be well fit with the single-component diffusion function over the entire composition range of these bilayers. Figure 3 shows the results of double-

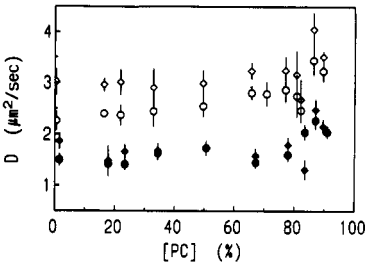

FIGURE 2: Dependence of the lipid lateral diffusion coefficients D on the total PC:PG composition in the second leaflet of the supported bilayer. The lateral diffusion coefficients were obtained from single-exponential fits of the FRAP curves with 1–1.5 mol % of NBD-PC (filled symbols) or NBD-PG (open symbols) as fluorescent probes. Circles (○, ●) correspond to diffusion coefficients measured in buffer containing 2 mM $CaCl_2$, and diamonds (◇, ◆) correspond to diffusion coefficients measured in buffer containing 1 mM EDTA.

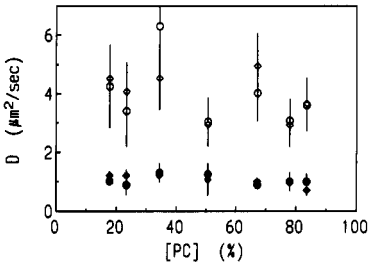

FIGURE 3: Dependence of the lateral diffusion coefficients of NBD-PC on the total PC:PG composition analyzed by double-exponential fits of the FRAP data. The open symbols represent the larger diffusion coefficient, D_1, and the filled symbols represent the smaller diffusion coefficient, D_2, in each sample. For other details, see the legend to Figure 2.

exponential fits of some of the same data on NBD-PC diffusion that were presented in Figure 2. The membranes with total PC contents of less than 15 mol % or more than 85 mol % exhibited single-exponential recoveries with no sign of a second component. Between 15 and 85 mol % PC, two components could clearly be resolved, one averaging about 1 $\mu m^2/s$ and the other about 4 $\mu m^2/s$. Within the error limits of these measurements the values of the two diffusion coefficients and their relative amplitudes (the mobile fractions were approximately 60% and 40% for the slower and faster components, respectively) did not appear to change within this entire composition range.

To evaluate the effects of annexin IV binding on the lateral diffusion of the lipids in supported bilayers, it was important to show that all protein-induced effects were reversible. Therefore, the lateral diffusion of the lipids was also routinely measured after annexin IV had been dissociated from the membranes with 1 mM EDTA (see Materials and Methods). The results of these experiments are listed in Table 1. It is seen from this table that the values of the lateral diffusion coefficients and the mobile fractions are absolutely reversible under all conditions in both the presence and absence of 2 mM Ca^{2+}.

Effects of Annexin IV Binding on Lateral Lipid Diffusion. Two representative FRAP curves of NBD-PG diffusion in the presence of approximately 120 nM annexin IV and 2 mM $CaCl_2$ are presented in Figure 4, panels A and B. The lipid compositions were 66:34 POPC:PG in Figure 4A and 16.5:83.5 POPC:PG in Figure 4B, respectively. The major differences between the two experiments are the longer time scale of diffusion and the deviation from a single exponential at the higher PG density (note that 50 and 75 lines per inch Ronchi rulings were used in the experiments of panels A and B of Figure 4, respectively). A single-exponential function

Table 1: Reversibility of the Lateral Diffusion Coefficients and the Mobile Fractions of the Lipids in Supported Planar Bilayers after Binding of Annexin IV

			D_{in}/D_{fin}[b]		mf_{in}/mf_{fin}[b]	
[PC] (mol %)	lipid probe	no. of samples[a]	1 mM EDTA	2 mM $CaCl_2$	1 mM $CaCl_2$	2 mM EDTA
89.6 ± 0.9	NBD-PG	5	0.93 ± 0.06	0.92 ± 0.06	1.01 ± 0.03	1.01 ± 0.03
82.2 ± 1.7	NBD-PG	10	0.99 ± 0.13	0.97 ± 0.10	1.01 ± 0.05	0.99 ± 0.06
80.8 ● 1.7	NBD-PG	7	0.99 ± 0.13	0.96 ± 0.12	1.05 ± 0.06	1.00 ± 0.08
65.8 ± 2.2	NBD-PG	8	0.96 ± 0.07	0.96 ± 0.07	1.00 ± 0.03	1.02 ± 0.03
32.9 ± 2.1	NBD-PG	9	0.98 ± 0.11	0.96 ± 0.08	0.99 ± 0.03	0.99 ± 0.02
16.4 ± 1.3	NBD-PG	6	0.97 ± 0.08	0.93 ± 0.05	0.98 ± 0.04	0.99 ± 0.03
91.0 ± 0.9	NBD-PC	4	1.09 ± 0.08	1.00 ± 0.11	0.97 ± 0.04	1.00 ± 0.04
17.8 ± 1.3	NBD-PC	4	1.03 ± 0.06	0.97 ± 0.08	1.02 ± 0.06	1.05 ± 0.04

[a] Number of independently prepared samples averaged. [b] The indices "in" and "fin" denote the best fit values of D and mf before annexin IV binding and after its removal by 1 mM EDTA treatment.

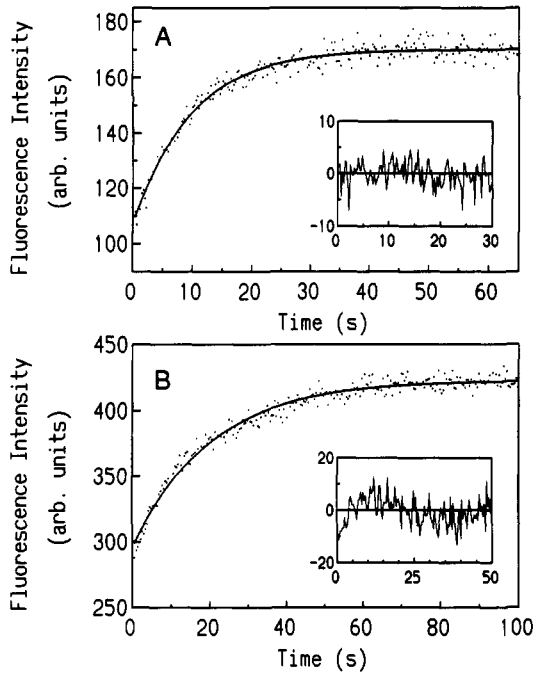

FIGURE 4: FRAP experiments measuring lipid diffusion in supported planar bilayers in the presence of annexin IV and 2 mM $CaCl_2$. The lipid compositions of the second leaflet of the supported bilayer were 66% POPC, 33% POPG, and 1.3% NBD-PG in (A) and 16% POPC, 83% POPG, and 1.3% NBD-PG in (B). The sample of panel A was measured in the presence of 125 nM annexin IV after three successive incubations with annexin IV for a total of 2.5 h (see Materials and Methods). The sample of panel B was measured in the presence of 116 nM annexin IV after 1-h incubation with annexin IV. Both curves were fit with a single-exponential function (lines), and the residuals between the experimental data and fitted curves are shown in the insets. The resulting lateral diffusion coefficients and mobile fractions were 0.42 $\mu m^2/s$ and 92% in (A) and 9.0×10^{-2} $\mu m^2/s$ and 100% in (B). The Ronchi rulings that were used were 50 lines per inch in (A) and 75 lines per inch in (B). The buffer was 10 mM Tris-HCl, pH 7.5, 0.1 M NaCl, and 2 mM $CaCl_2$.

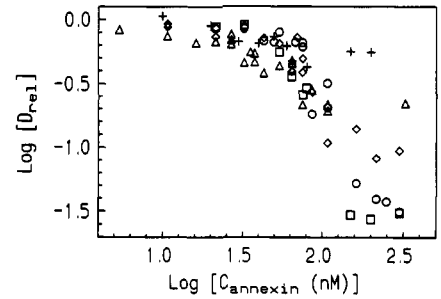

FIGURE 5: Dependence of the relative lipid diffusion coefficient $D_{rel} = D/D_0$ on the annexin IV concentration. D and D_0 are the lateral diffusion coefficients of 1–1.5 mol % NBD-PG derived from single- or double exponential fits in the presence and absence of annexin IV, respectively. When two diffusion components were observed (at high annexin concentrations, see Figure 6), the smaller diffusion coefficient is plotted. The POPC:PG molar ratios in the second leaflet of the SPB were 90:10 (+), 82:18 (△), 66:34 (◇), 33:67 (○), and 16:84 (□). The buffer was 0.01 M Tris-HCl, pH 7.5, 0.1 M NaCl, and 2 mM $CaCl_2$.

was sufficient to fit the data of Figure 4A, whereas the data of Figure 4B could only be fit satisfactorily with a double-exponential function (see insets showing the residuals after single-exponential fits in both cases). The numerical values of the derived diffusion coefficients and mobile fractions (averaged from several identically prepared samples) were $(4.3 \pm 0.1) \times 10^{-1}$ $\mu m^2/s$ and 97 ± 1% at 66 mol % PC, and $(4.7 \pm 0.6) \times 10^{-2}$ $\mu m^2/s$, 79 ± 4%, and $(5.1 \pm 2.2) \times 10^{-1}$ $\mu m^2/s$, 21 ± 4% at 16.5 mol % PC, respectively. Apparently, annexin IV exerts two distinct effects on the diffusion of NBD-PG when it binds to mixed POPC:PG membranes: (1) it reduces the rate of lateral diffusion of the lipid probe, and (2) it induces two different environments for this probe, which diffuse at two different rates under some, but not all, conditions of PC:PG:annexin IV composition.

In order to establish how these two effects depend on the PC:PG composition, it was necessary to first measure the dependence of the lateral diffusion coefficients on the annexin IV concentration at each PC:PG composition. These data are shown in double logarithmic plots in Figure 5. Whenever double-exponential recoveries were observed, the smaller of the two diffusion coefficients is plotted in this figure. It follows from an inspection of Figure 5 that annexin IV binding was able to reduce the lateral diffusion coefficients of NBD-PG at all lipid compositions and that this reduction became increasingly more effective with increasing PG densities in the membrane. However, the transition from the rapidly diffusing state to the slowly diffusing state occurred at about 80 nM annexin IV, independent of the membrane composition.

At about 80 nM annexin IV an onset of a two-component diffusion behavior of NBD-PG was observed in bilayers of some, but not all, POPC:POPG compositions. Three representative titrations are presented in Figure 6. Up to 80 nM annexin, lateral diffusion was always single-component, even though the diffusion coefficients decreased slightly in this range of annexin IV concentration. The single-component behavior further persisted up to high annexin IV concentrations at intermediate densities of PG in mixed POPC:POPG bilayers. For example, at 66 mol % PC, only the measurements at the last concentration point (198 nM annexin IV) could be reliably resolved into two components (Figure 6B). In contrast, two-component diffusion was more prominently expressed at high, i.e., 90 mol % (Figure 6A), or low, i.e., 16 mol % (Figure 6C), PC densities in the bilayer. The two diffusion coefficients,

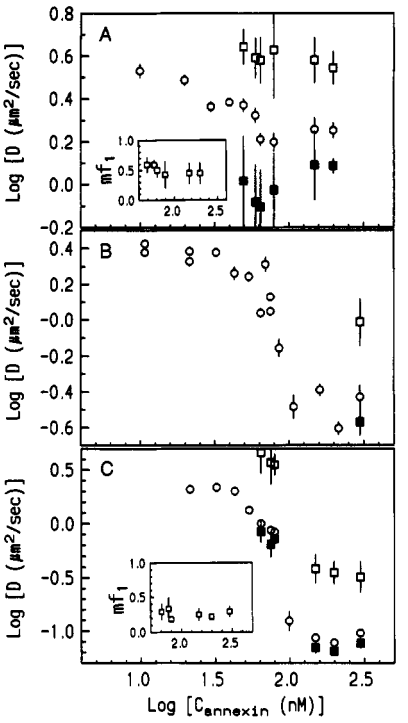

FIGURE 6: Dependence of the lateral diffusion coefficient D of 1–1.5 mol % NBD-PG on the annexin IV concentration, at three different POPC:PG ratios, namely, 90:10 (A), 66:34 (B), and 16:84 (C). The circles (○) represent lateral diffusion coefficients that were obtained by fitting the data to single exponentials. For those cases where a fit by a single exponential was not satisfactory (see text), the data were fit to a double-exponential function. The open squares (□) represent the larger lateral diffusion coefficients, and the filled squares (■) represent the smaller lateral diffusion coefficients at each annexin IV concentration and lipid composition. The mobile fractions of the component with the larger diffusion coefficient (mf_1) are shown in the insets of panels A and C. The buffer was 0.01 M Tris-HCl, pH 7.5, 0.1 M NaCl, and 2 mM $CaCl_2$.

which each accounted for about 50% of the entire mobile fraction, were about 4.0 and about 1.0 $\mu m^2/s$ at 90 mol % PC. The error bars are relatively large in these deconvolutions because of the small (3- to 4-fold) difference between the two diffusion coefficients. At 16 mol % PC, both D_1 and D_2 were smaller, and the difference between them was somewhat larger. D_1 was about 0.33 $\mu m^2/s$ (25% of the total mobile fraction), and D_2 was about 0.07 $\mu m^2/s$.

The dependences of the lateral diffusion coefficients on the annexin IV concentrations were also measured with the NBD-PC probe at PC mole fractions of 91 and 18 mol % (data not shown). Quite similar results were obtained as with the NBD-PG probe, except that two diffusion components could be resolved with this probe at all annexin IV concentrations. This is not surprising, because the diffusion measurements with this probe resulted in biphasic recoveries even in the absence of annexin IV (see above).

Figure 7 summarizes the lateral diffusion coefficients as a function of the lipid composition in the bilayer *at saturating annexin IV concentrations*. All FRAP curves could be resolved into two components under these conditions, and both D_1 and D_2 are plotted in Figure 7. Interestingly, the dependences of the charged and uncharged lipid probes parallel each other over the entire composition range of PC:PG in the bilayer. The smallest lateral diffusion coefficients were observed in pure POPG membranes with only 1.5 mol % of either of the two fluorescent lipid probes present. These diffusion coefficients were $D_1 = (4.7 \pm 0.5) \times 10^{-1}$ $\mu m^2/s$ and $D_2 = (6.7 \pm 0.3) \times 10^{-2}$ $\mu m^2/s$ for NBD-PG, and $D_1 = (3.2 \pm 1.3) \times 10^{-1}$ $\mu m^2/s$ and $D_2 = (2.2 \pm 0.2) \times 10^{-2}$ $\mu m^2/s$ for NBD-PC, respectively. These values correspond to reductions of 5.0-, 35-, 4.4-, and 64-fold, respectively, from the corresponding diffusion coefficients in the absence of annexin IV and the presence of 2 mM $CaCl_2$. These diffusion coefficients remained approximately constant up to equimolar concentrations of PC and PG and increased gradually at higher PC (lower PG) densities in the bilayer.

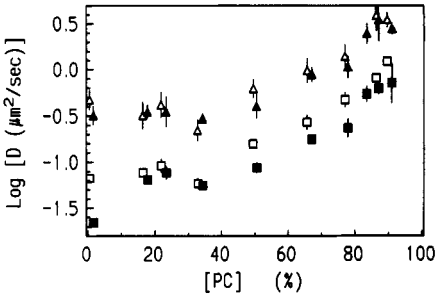

FIGURE 7: Dependence of the lipid lateral diffusion coefficients D_1 (△, ▲) and D_2 (□, ■) on the total PC:PG composition in the second leaflet of the supported bilayer. All data were measured in the presence of saturating annexin IV concentrations, i.e., 180–320 nM annexin IV. The fluorescent lipid probes were either 1–1.5 mol % NBD-PG (open symbols) or 1–1.5 mol % NBD-PC (filled symbols). The buffer was 0.01 M Tris-HCl, pH 7.5, 0.1 M NaCl, and 2 mM $CaCl_2$. Note the logarithmic scale of the ordinate.

DISCUSSION

When annexin IV binds to planar supported lipid bilayers in the presence of Ca^{2+}, it decreases the lateral diffusion coefficients of the constituent lipids by large factors. In bilayers composed of POPC and POPG, lateral lipid diffusion coefficients of the order of 2.5 and 1.6 $\mu m^2/s$ were measured with the chain-labeled fluorescent lipid analogs NBD-PG and NBD-PC, respectively, in the absence of annexin IV and the presence of 2 mM Ca^{2+}. The population of NBD-PG appears to be homogeneous with a single lateral diffusion coefficient under these conditions. However, when saturating amounts of annexin IV are added to these bilayers, two populations of NBD-PG are observed, which both diffuse at lower rates. The two diffusion coefficients are approximately 0.5 and 0.07 $\mu m^2/s$, which corresponds to a 5- and 35-fold reduction of the lipid diffusion coefficient in the absence of annexin IV. The faster component comprises about 20–30% and the slower component about 70–80% of all NBD-PG molecules in the membrane. Therefore, we conclude that under appropriate conditions annexin IV is able to induce two phases of different composition in these lipid bilayers. NBD-PG apparently is able to partition into both phases. Whether these phases distinguish themselves with respect to their lipid composition or with respect to the annexin IV:lipid ratio, or both, cannot be decided on the basis of the present experiments.

The lateral diffusion coefficient of 0.07 $\mu m^2/s$ is one of the smallest diffusion coefficients that has been reported for any fluid-phase lipid in lipid model systems or biological membranes. Integral membrane proteins usually do not retard lateral lipid diffusion more than about 5- to 10-fold, even at the highest protein densities (Peters & Cherry, 1982; Beck, 1987). Membrane-surface binding proteins, such as antibodies or a prothrombin fragment, reduced lateral lipid diffusion coefficients only 1- to 4-fold (Tamm, 1988; Huang et al., 1992). On the other hand, lateral diffusion coefficients of lipids in the gel ($L_{\beta'}$) phase are still smaller (by at least 2 orders of magnitude) than the smallest lateral diffusion coefficient reported in this work (Tamm & McConnell, 1985).

Therefore, although the lateral diffusion coefficient of one component is rather low in the presence of bound annexin, we believe that both phases still consist of fluid phase-like lipids. The smaller of the two diffusion coefficients is in the same range as that measured in pure lipid systems with cholesterol under some conditions (Rubenstein et al., 1979; Almeida et al., 1993). The larger diffusion coefficient (0.5 $\mu m^2/s$) is very similar to the diffusion coefficient of NBD-PS when prothrombin fragment 1 is bound to planar membranes composed of 30% bovine brain PS and 70% POPC in the presence of Ca^{2+} (Huang et al., 1992).

NBD-PC exhibits two lateral diffusion components in supported bilayers composed of POPC and POPG, even in the absence of annexin IV. We observe two-component diffusion in the entire compositional range between 15 and 85 mol % of PC. However, there is no sign of two components when the outer leaflets of the supported bilayer are pure PG or pure PC, or when they contain less than 15 mol % of the minor lipid. A possible explanation for the double-exponential recovery of NBD-PC is that this lipid could flip into the pure POPC leaflet of the bilayer adjacent to the substrate where its lateral diffusion coefficient is slightly reduced (Kalb et al., 1992). This is not possible for NBD-PG because negatively charged lipids are repelled by the weakly negatively charged silicon dioxide substrate. Other explanations may account for the two fast diffusion coefficients of the NBD-PC probe (approximately 4 and 1 $\mu m^2/s$), but our experiments were not designed to resolve this question. Also, the result that we find two fast diffusion coefficients with this probe does not affect our conclusions on the fluid-phase structure of the membranes with bound annexin IV, since the reduction of the lateral diffusion coefficients of the NBD-PC probe is essentially the same as for the NBD-PG probe. Again, two diffusion coefficients are observed with NBD-PC which are approximately 5- and 40-fold reduced from the diffusion coefficients in the absence of annexin IV. In the presence of bound annexin IV, biphasic lateral diffusion is not limited to the 15–85 mol % range of PC in the mixed bilayers, but extends to the nearly pure PG bilayers.

The fact that NBD-PC and NBD-PG diffusion are so similar to each other in the presence of bound annexin IV argues against a selective and stoichiometric binding of a significant fraction of the PG molecules to the membrane-binding face of annexin IV. We rather view the binding as a strong, nonstoichiometric binding of two complementary surfaces, namely, the convex face of annexin and the liquid-crystalline surface of the lipid bilayer. From direct binding studies of annexin V to anionic lipid vesicles it is known that a significant part of the interaction force is electrostatic, because annexin binding to mixed PC:PS membranes can be partially screened by NaCl (Tait et al., 1989). If the Ca^{2+}-binding face of annexin becomes only lipid-binding when the Ca^{2+} sites are occupied, the observed electrostatic effect may be indirect, because the Ca^{2+} concentration is much higher near a negatively charged membrane surface than in bulk solution. Steric and hydrophobic interactions may also contribute to the binding of some annexins to lipid bilayers. For instance, membranes of PEs which lack the bulky methyl groups of the PCs on their headgroup terminal amines bind annexins more strongly than PCs in otherwise identical membranes (Andree et al., 1990), and a conformational change which involves the exposure of a tryptophan residue toward the membrane surface has been shown to occur when one particular Ca^{2+} binding site becomes occupied in annexin V (Meers, 1990; Concha et al., 1993). Our lateral diffusion experiments do not permit us to dissect the various interactions that could contribute to annexin–membrane binding, but they are sufficient to exclude a simple stoichiometric binding of acidic lipids to individual annexin molecules with independent binding sites.

Details of the composition, geometric arrangement, and internal nature of the two coexisting fluid phases cannot be directly obtained from the data presented in this work. For instance, we do not know whether the annexins bind to only one or both of the two lipid phases. Nevertheless, we can reach conclusions on some properties of the two phases. The most simple-minded interpretation of the reduced lateral diffusion coefficients as measured by FRAP is perhaps that the lipid lateral diffusion coefficients within each fluid phase might have changed after binding of annexin IV. We consider this possibility unlikely, because for this case we would expect that the lateral diffusion coefficients of the lipids would change by similar factors when determined by a technique that (unlike FRAP) measures lateral diffusion on a small length scale. This however was not observed. When lateral diffusion was measured with pyrene-labeled PGs in mixed PC:PG vesicles by eximer formation which is sensitive to short-range lateral diffusion (the length scale of this experiment is of the order of 1 to a few nm), a 30% decrease of the eximer-to-monomer equilibrium was observed after annexin IV had been bound to these vesicles in the presence of Ca^{2+} (Junker & Creutz, 1993). This decrease can be interpreted with a decrease of the short-range lateral diffusion coefficient of not more than 2-fold.

Next, we consider models that involve the formation of lipid domains in the bilayer after annexin binding. Our attempts to directly detect lipid domains by fluorescence microscopy were unsuccessful. Therefore, the domains must be smaller than the spatial resolution of our imaging system, i.e., smaller than about 400 nm, or both probes must partition equally between the two kinds of domains so that no contrast is achieved. On the other hand, our FRAP experiments measure diffusive lipid transport over distances of several micrometers for both components. No significant immobile fractions were observed in all of our experiments. These two observations leave us with two plausible domain models, i.e., one that allows for exchange of lipids between domains and one that does not.[2] In both cases the 5-fold reduced diffusion coefficient is explained by diffusion of unrestricted lipid which, however, is hindered in its free path by obstacles posed by membrane domains of different composition or physical properties. This effect has been studied theoretically and experimentally in great detail [Saxton, 1987; Almeida et al. (1993) and references cited therein] and pictorially has been termed "diffusion in an archipelago". If lipids can exchange

[2] A reviewer has suggested an extension of our domain model with lipid exchange. In Figure 6, it will be noted that the slow diffusion coefficient at low PG (panel A) is approximately equal to the fast diffusion coefficient at high PG (panel C). Therefore, one might assign this diffusion coefficient to the same molecular process, e.g., the rate of NBD-PG exchanging between annexin-rich and annexin-poor domains. In the case of low PG, annexin-rich domains are expected to be sparse, even at saturating annexin concentration, and the fast diffusion coefficient would represent free probe diffusion in the remaining areas. In the case of high PG, most of the membrane surface would be covered with annexin, and lipid diffusion in this domain would be slow (slower than lipid exchange). However, this model breaks down for the data of Figure 7, where the diffusion coefficients at saturating annexin concentration are followed over the entire PC:PG compositional range. If the model were correct, one would expect one constant diffusion coefficient at about 3×10^{-9} cm^2/s (–0.5 on our log scale) and a crossover of this line by the other diffusion coefficient. This is not experimentally observed. The fast and slow diffusion coefficients both change monotonically in this plot.

between, for example, an annexin-rich and an annexin-poor domain on a time scale of milliseconds to seconds (i.e., faster than the time scale of the FRAP experiment and slower than by unrestricted diffusion), their effective long-range diffusion coefficient can be retarded quite significantly and could easily account for the 35- to 40-fold reduction of the lateral diffusion coefficient. On the other hand, if lipid exchange does not occur, the smaller diffusion coefficient could be representative of the diffusion of an entire annexin-rich domain in the fluid lipid bilayer. According to the Saffmann–Delbrück equation (Saffmann & Delbrück, 1972), which describes the size dependence of the lateral diffusion of individual proteins or protein oligomers in lipid bilayers,[3] the size of the slowly diffusing domains would be of the order of 100–200 nm in membranes of high PG content. Although our present lateral diffusion experiments cannot distinguish between these two domain models, it is clear that annexin has changed the fluid-phase structure and the overall fluid-mechanical properties of the lipid bilayer.

CONCLUSION

We have found that annexin IV reduces the lateral diffusion coefficients of lipids and changes the fluid-phase structure in lipid bilayers when it binds to membranes that contain the negatively charged lipid POPG in the presence of 2 mM Ca^{2+}. The annexins have traditionally been viewed as exhibiting a high degree of specificity for binding to negatively charged phospholipids and phosphatidylethanolamines rather than phosphatidylcholines. However, our results demonstrate that once an annexin is bound to a membrane with a net negative surface charge, the behavior of the phosphatidylcholines is also profoundly altered. It will be interesting to see whether this effect is directly related to the formation of lipid clusters that has been reported to occur in PC:PA or PE:PA bilayers after binding of annexin VI (Bazzi & Nelsestuen, 1992). A redistribution and restructuring of lipids in membranes as a consequence of annexin binding may be an important component of one of the proposed functions of some annexins, namely, to prepare secretory vesicles and plasma membranes for fusion in exocytosis.

ACKNOWLEDGMENT

We thank Dr. Peter Hinterdorfer for his help with the FRAP instrumentation and helpful discussions. We also thank Ms. Sandy Snyder for her help with the growth of the cell cultures and protein purification.

REFERENCES

Almeida, P. F. F., Vaz, W. L. C., & Thompson, T. E. (1993) *Biophys. J. 64*, 399–412.

Andree, H. A. M., Reutelingsperger, C. P. M., Hauptmann, R., Hemker, H. C., Hermens, W. T., & Williams, G. M. (1990) *J. Biol. Chem. 265*, 4923–4928.

Bazzi, M. D., & Nelsestuen, G. L. (1991) *Biochemistry 30*, 7961–7969.

Bazzi, M. D., & Nelsestuen, G. L. (1992) *Biochemistry 31*, 10406–10413.

Bazzi, M. D., Youakim, M. A., & Nelsestuen, G. L. (1992) *Biochemistry 31*, 1125–1134.

Beck, K. (1987) Cytomechanics. *The Mechanical Basis of Cell Form and Structure*. Bereitner-Hahn, J., Anderson, O. R., & Reif, W.-E., Eds.) pp 79–99, Springer-Verlag, Berlin, pp 79–99.

Concha, N. O., Head, J. F., Kaetzel, M. A., Dedman, J. R., & Seaton, B. A. (1992) *FEBS Lett. 314*, 159–162.

Concha, N. O., Head, J. F., Kaetzel, M. A., Dedman, J. R., & Seaton, B. A. (1993) *Science 261*, 1321–1324.

Creutz, C. E. (1992) *Science 258*, 924–931.

Creutz, C. E., Snyder, S. L., & Kambouris, N. G. (1991) *Yeast 7*, 229–244.

Hamman, H. C., Gaffey, L. C., Lynch, K. R., & Creutz, C. E. (1988) *Biochem. Biophys. Res. Commun. 156*, 660–667.

Huang, Z., Pearce, K. H., & Thompson, N. L. (1992) *Biochim. Biophys. Acta 1112*, 259–265.

Huber, R., Römisch, J., & Paques, E.-P. (1990) *EMBO J. 9*, 3867–3874.

Huber, R., Berendes, R., Burger, A., Schneider, M., Karshikov, A., Luecke, H., Römisch, J., & Paques, E. (1992) *J. Mol. Biol. 223*, 683–704.

Junker, M., & Creutz, C. E. (1993) *Biochemistry 32*, 9968–9974.

Kalb, E., Frey, S., & Tamm, L. K. (1992) *Biochim. Biophys. Acta 1103*, 307–316.

Meers, P. (1990) *Biochemistry 29*, 3325–3330.

Meers, P., Bentz, J., Alford, D., Nir, S., Papahadjopoulos, D., & Hong, K. (1988) *Biochemistry 27*, 4430–4439.

Meers, P., Daleka, D., Hong, K., & Papahadjopoulos, D. (1991) *Biochemistry 30*, 2903–2908.

Meers, P., Mealy, T., Parlotsky, N., & Tauber, A. I. (1992) *Biochemistry 31*, 6372–6382.

Mosser, G., Ravanat, C., Freyssinet, J.-M., & Brisson, A. (1991) *J. Mol. Biol. 217*, 241–245.

Nelson, M. K. (1993) Ph.D. Thesis, University of Virginia.

Newman, R. H., Tucker, A., Ferguson, C., Tsernoglou, D., Leonard, K., & Crumpton, M. J. (1989) *J. Mol. Biol. 206*, 213–219.

Newman, R. H., Leonard, K., & Crumpton, M. J. (1991) *FEBS Lett. 279*, 21–24.

Peters, R., & Cherry, R. J. (1982) *Proc. Natl. Acad. Sci. U.S.A. 79*, 4317–4321.

Rubenstein, J. L. R., Smith, B. A., & McConnell, H. M. (1979) *Proc. Natl. Acad. Sci. U.S.A. 76*, 15–18.

Saffmann, D. G., & Delbrück, M. (1975) *Proc. Natl. Acad. Sci. U.S.A. 72*, 3111–3113.

Saxton, M. J. (1987) *Biophys. J. 52*, 989–997.

Smith, B. A., & McConnell, H. M (1978) *Proc. Natl. Acad. Sci. U.S.A. 75*, 2759–2763.

Studier, F. W., Rosenberg, A. H., Dunn, J. J., & Dubendorff, J. W. (1990) *Methods Enzymol. 185*, 60–89.

Tait, J. F., Gibson, D., & Fujikawa, K. (1989) *J. Biol. Chem. 264*, 7944–7949.

Tamm, L. K. (1988) *Biochemistry 27*, 1450–1457.

Tamm, L. K., & McConnell, H. M. (1985) *Biophys. J. 47*, 105–113.

Tamm, L. K., & Kalb, E. (1993) in *Molecular Luminescence Spectroscopy, Part 3* (Schulman, S. G., Ed.) Chemical Analysis Series, Vol. 77, pp 253–305, John Wiley and Sons, N.Y.

Weng, X., Luecke, H., Sung, I. S., Kang, O. X., Kim, S.-H., & Huber, R. (1993) *Protein Sci. 2*, 448–458.

Zaks, W. J., & Creutz, C. E. (1991) *Biochemistry 30*, 9607–9615.

[3] This calculation of domain sizes should only be taken as a qualitative order of magnitude estimate, because the validity of the Saffmann–Delbrück equations has never been tested experimentally with very large protein aggregates or membrane domains.